

# Thermo Electric Sensitivity Fractal Dimension for Characterizing Shajara Reservoirs of the Permo-Carboniferous Shajara Formation, Saudi Arabia

Khalid Elyas Mohamed Elameen Alkhidir

Department of Petroleum and Natural Gas Engineering,  
College of Engineering, King Saud University, Saudi Arabia

## \*Corresponding author

Khalid Elyas Mohamed Elameen Alkhidir, Department of Petroleum and Natural Gas Engineering, College of Engineering, King Saud University, Saudi Arabia, Email: kalkhidir@ksu.edu.sa

Submitted: 21 May 2019; Accepted: 27 May 2019; Published: 30 May 2019

## Abstract

The quality and assessment of a reservoir can be documented in details by the application of thermo electric sensitivity. This research aims to calculate fractal dimension from the relationship among thermo electric sensitivity, maximum thermo electric sensitivity and wetting phase saturation and to approve it by the fractal dimension derived from the relationship among capillary pressure and wetting phase saturation. Two equations for calculating the fractal dimensions have been employed. The first one describes the functional relationship between wetting phase saturation, thermo electric sensitivity, maximum Thermo electric sensitivity and fractal dimension. The second equation implies to the wetting phase saturation as a function of capillary pressure and the fractal dimension. Two procedures for obtaining the fractal dimension have been utilized. The first procedure was done by plotting the logarithm of the ratio between thermo electric sensitivity and maximum thermo electric sensitivity versus logarithm wetting phase saturation. The slope of the first procedure =  $3 - D_f$  (fractal dimension). The second procedure for obtaining the fractal dimension was determined by plotting the logarithm of capillary pressure versus the logarithm of wetting phase saturation. The slope of the second procedure =  $D_f - 3$ . On the basis of the obtained results of the fabricated stratigraphic column and the attained values of the fractal dimension, the sandstones of the Shajara reservoirs of the Shajara Formation were divided here into three units.

**Keywords:** Shajara Reservoirs, Shajara Formation, Thermo Electric Sensitivity Fractal Dimension, Capillary Pressure Fractal Dimension

## Introduction

Seismo electric effects related to electro kinetic potential, dielectric permittivity, pressure gradient, fluid viscosity, and electric conductivity was first reported by [1]. Capillary pressure follows the scaling law at low wetting phase saturation was reported by [2]. Seismo electric phenomenon by considering electro kinetic coupling coefficient as a function of effective charge density, permeability, fluid viscosity and electric conductivity was reported by [3]. The magnitude of seismo electric current depends on porosity, pore size, zeta potential of the pore surfaces, and elastic properties of the matrix was investigated by [4]. The tangent of the ratio of converted electric field to pressure is approximately in inverse proportion to permeability was studied by [5]. Permeability inversion from seismo electric log at low frequency was studied by [6]. They reported that, the tangent of the ratio among electric excitation intensity and pressure field is a function of porosity, fluid viscosity, frequency, tortuosity, fluid density and Dracy permeability. A decrease of seismo electric frequencies with increasing water content was reported by [7]. An increase of seismo electric transfer function with increasing water saturation was studied by [8]. An increase of dynamic seismo electric transfer function with decreasing fluid conductivity was described by [9]. The amplitude

of seismo electric signal increases with increasing permeability which means that the seismo electric effects are directly related to the permeability and can be used to study the permeability of the reservoir was illustrated by [10]. Seismo electric coupling is frequency dependent and decreases exponentially when frequency increases was demonstrated by [11]. An increase of permeability with increasing pressure head and bubble pressure fractal dimension was reported by [12, 13]. An increase of geometric relaxation time of induced polarization fractal dimension with permeability increasing and grain size was described by [14, 15].

## Materials and Methods

Sandstone samples were collected from the surface type section of the Permo-Carboniferous Shajara Formation, latitude  $26^{\circ} 52' 17.4''$ , longitude  $43^{\circ} 36' 18''$ . (Figure1). Porosity was measured on collected samples using mercury intrusion Porosimetry and permeability was derived from capillary pressure data. The purpose of this paper is to obtain thermo electric sensitivity fractal dimension and to confirm it by capillary pressure fractal dimension. The fractal dimension of the first procedure is determined from the positive slope of the plot of logarithm of the ratio of thermo electric sensitivity to maximum thermo electric sensitivity  $\log(TES^{1/2}/TES^{1/2}_{max})$  versus  $\log$  wetting phase saturation ( $\log Sw$ ). Whereas the fractal dimension of the second procedure is determined from the negative slope of the plot of logarithm of  $\log$  capillary pressure ( $\log Pc$ ) versus logarithm of

wetting phase saturation (log Sw).

The thermo electric sensitivity can be scaled as

$$Sw = \left[ \frac{TES^1}{TES_{max}^{1/2}} \right]^{[3-Df]} \quad 1$$

Where Sw the water saturation, TES thermo electric sensitivity in volt / kelvin, TESmax the maximum thermo electric sensitivity in volt / kelvin, and Df the fractal dimension.

Equation 1 can be proofed from

$$reff^2 = \left[ \frac{8 * \sigma * \eta * Cs}{CE} \right] \quad 2$$

Where reff the effective pore radius in meter,  $\sigma$  the electric conductivity in Siemens / meter,  $\eta$  the viscosity in pascal \* second, Cs the streaming potential coefficient in volt / pascal, and CE the electro osmosis coefficient in pascal / volt.

The streaming potential coefficient CS can be scaled as

$$CS = \left[ \frac{\Delta V}{\Delta P} \right] \quad 3$$

Where CS the streaming potential coefficient in volt / pascal,  $\Delta V$  the differential potential in volt, and  $\Delta P$  the differential pressure in pascal.

Insert equation 3 into equation 2

$$reff^2 = \left[ \frac{8 * \sigma * \eta * \Delta V}{CE * \Delta P} \right] \quad 4$$

The differential pressure can be scaled as

$$\Delta V = TES * \Delta T \quad 5$$

Where  $\Delta V$  the differential potential in volt, TES thermos electric sensitivity in volt / kelvin and T the differential temperature in kelvin. Insert equation 5 into equation 4

$$reff^2 = \left[ \frac{8 * \sigma * \eta * TES * \Delta T}{CE * \Delta P} \right] \quad 6$$

The maximum thermos electric sensitivity TESmax can be scaled as

$$reff_{max}^2 = \left[ \frac{8 * \sigma * \eta * TES_{max} * \Delta T}{CE * \Delta P} \right] \quad 7$$

Divide equation 6 by equation 7

$$\left[ \frac{reff^2}{reff_{max}^2} \right] = \left[ \frac{\left[ \frac{8 * \sigma * \eta * TES * \Delta T}{CE * \Delta P} \right]}{\left[ \frac{8 * \sigma * \eta * TES_{max} * \Delta T}{CE * \Delta P} \right]} \right] \quad 8$$

Equation 8 after simplification will become

$$\left[ \frac{reff^2}{reff_{max}^2} \right] = \left[ \frac{TES}{TES_{max}} \right] \quad 9$$

Take the square root of equation 9

$$\sqrt{\left[ \frac{reff^2}{reff_{max}^2} \right]} = \sqrt{\left[ \frac{TES}{TES_{max}} \right]} \quad 10$$

Equation 10 after simplification will become

$$\left[ \frac{reff}{reff_{max}} \right] = \left[ \frac{TES^{\frac{1}{2}}}{TES_{max}^{\frac{1}{2}}} \right] \quad 11$$

Take the logarithm of equation 11

$$\log \left[ \frac{reff}{reff_{max}} \right] = \log \left[ \frac{TES^{\frac{1}{2}}}{TES_{max}^{\frac{1}{2}}} \right] \quad 12$$

$$\text{But; } \log \left[ \frac{reff}{reff_{max}} \right] = \left[ \frac{\log SW}{3 - Df} \right] \quad 13$$

Insert equation 13 into equation 12

$$\left[ \frac{\log SW}{3 - Df} \right] = \log \left[ \frac{TES^{\frac{1}{2}}}{TES_{max}^{\frac{1}{2}}} \right] \quad 14$$

Equation 14 after log removal will become

$$SW = \left[ \frac{TES^{\frac{1}{2}}}{TES_{max}^{\frac{1}{2}}} \right]^{[3-Df]} \quad 15$$

Equation 15 the proof of equation 1 which relates the water saturation, thermos electric sensitivity, maximum thermos electric sensitivity and the fractal dimension.

The capillary pressure can be scaled as

$$Sw = [Df - 3] * Pc * \text{constant} \quad 16$$

Where Sw the water saturation, Pc the capillary pressure and Df the fractal dimension.

## Results and Discussion

Based on field observation the Shajara Reservoirs of the Permo-Carboniferous Shajara Formation were divided here into three units as described in Figure 1. These units from bottom to top are: Lower Shajara Reservoir, Middle Shajara reservoir, and Upper Shajara Reservoir. Their attained results of the Thermo electric sensitivity fractal dimension and capillary pressure fractal dimension are shown in Table 1. Based on the achieved results it was found that the Thermo electric sensitivity fractal dimension is equal to the capillary pressure fractal dimension. The maximum value of the fractal dimension was found to be 2.7872 allocated to sample SJ13 from the Upper Shajara Reservoir as verified in Table 1. Whereas the minimum value of the fractal dimension 2.4379 was reported from sample SJ3 from the Lower Shajara reservoir as shown in Table 1. The Thermo electric sensitivity fractal dimension and capillary pressure fractal dimension were detected to increase with increasing permeability as proofed in Table 1 owing to the possibility of having interconnected channels.

**Table 1: Petrophysical model showing the three Shajara Reservoir Units with their corresponding values of Thermo electric sensitivity fractal dimension and capillary pressure fractal dimension**

Formation	Reservoir	Sample	Porosity %	k (md)	Positive slope of the first procedure Slope=3-Df	Negative slope of the second procedure Slope=Df-3	Thermo electric sensitivity fractal dimension	Capillary pressure fractal dimension
Permo-Carboniferous Shajara Formation	Upper	SJ13	25	973	0.2128	-0.2128	2.7872	2.7872
	Shajara	SJ12	28	1440	0.2141	-0.2141	2.7859	2.7859
	Reservoir	SJ11	36	1197	0.2414	-0.2414	2.7586	2.7586
	Middle	SJ9	31	1394	0.2214	-0.2214	2.7786	2.7786
	Shajara	SJ8	32	1344	0.2248	-0.2248	2.7752	2.7752
	Reservoir	SJ7	35	1472	0.2317	-0.2317	2.7683	2.7683
	Lower	SJ4	30	176	0.3157	-0.3157	2.6843	2.6843
	Shajara	SJ3	34	56	0.5621	-0.5621	2.4379	2.4379
	Reservoir	SJ2	35	1955	0.2252	-0.2252	2.7748	2.7748
			SJ1	29	1680	0.2141	-0.2141	2.7859

The Lower Shajara reservoir was symbolized by six sandstone samples (Figure 1), four of which label as SJ1, SJ2, SJ3 and SJ4 were carefully chosen for capillary pressure measurement as proven in Table 1. Their positive slopes of the first procedure log of the Thermo electric sensitivity to maximum Thermo electric sensitivity versus log wetting phase saturation (Sw) and negative slopes of the second procedure log capillary pressure (Pc) versus log wetting phase saturation (Sw) are clarified in Figure 2, Figure 3, Figure 4, Figure 5 and Table 1. Their Thermo electric sensitivity fractal dimension and capillary pressure fractal dimension values are revealed in Table 1. As we proceed from sample SJ2 to SJ3 a pronounced reduction in permeability due to compaction was described from 1955 md to 56 md which reflects decrease in Thermo electric sensitivity fractal dimension from 2.7748 to 2.4379 as quantified in table 1. Again, an increase in grain size and permeability was proved from sample SJ4 whose Thermo electric sensitivity fractal dimension and capillary pressure fractal dimension was found to be 2.6843 as described in Table 1.

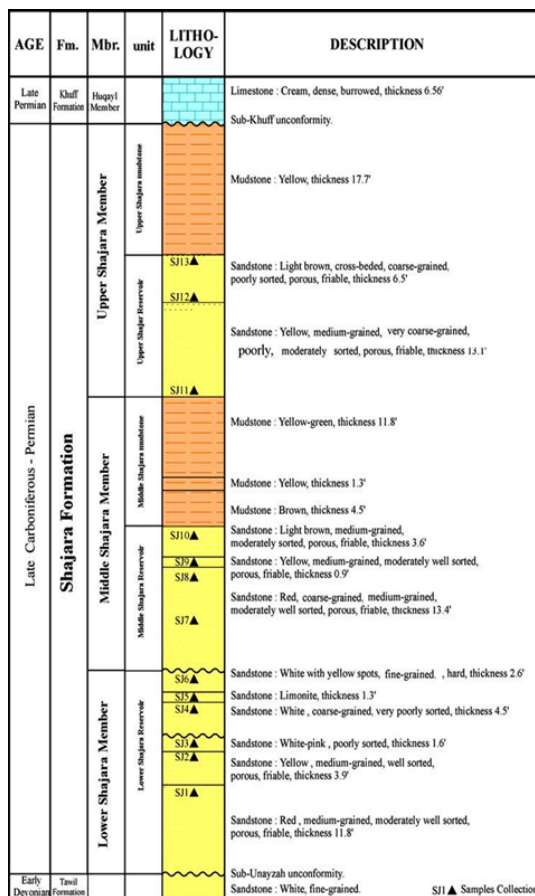


**Figure 1: Surface type section of the Shajara Reservoirs of the Permo-Carboniferous Shajara Formation at latitude 26° 52' 17.4" longitude 43° 36' 18"**

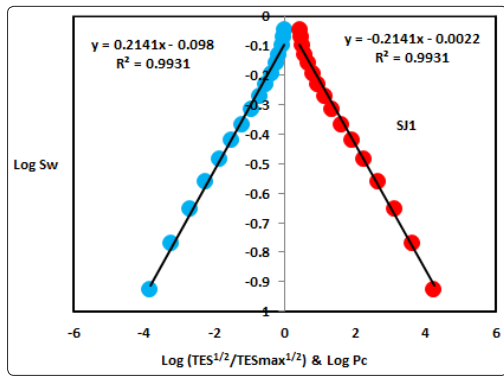


Figure 2:  $\text{Log} (TES^{1/2}/TES_{max}^{1/2})$  &  $\text{log pc}$  versus  $\text{log Sw}$  for sample SJ1

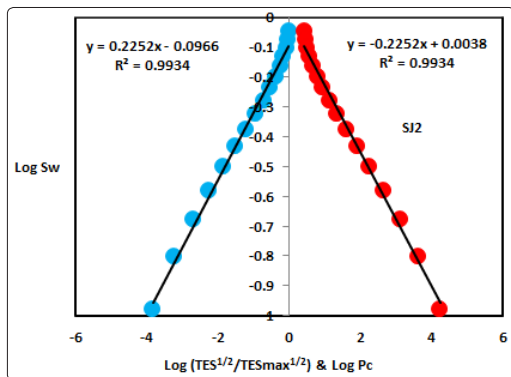


Figure 3:  $\text{Log} (TES^{1/2}/TES_{max}^{1/2})$  &  $\text{log pc}$  versus  $\text{log Sw}$  for sample SJ2

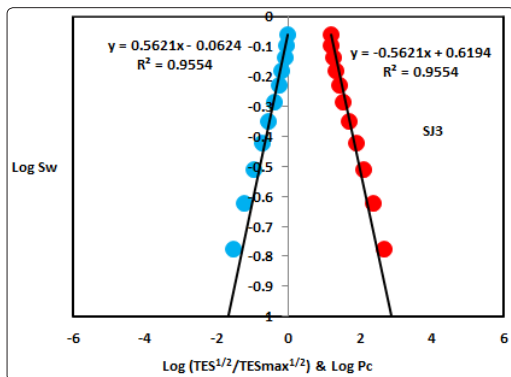


Figure 4:  $\text{Log} (TES^{1/2}/TES_{max}^{1/2})$  &  $\text{log pc}$  versus  $\text{log Sw}$  for sample SJ3

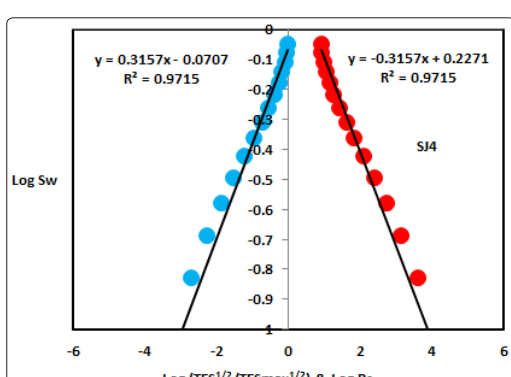


Figure 5:  $\text{Log} (TES^{1/2}/TES_{max}^{1/2})$  &  $\text{log pc}$  versus  $\text{log Sw}$  for sample SJ4

In contrast, the Middle Shajara reservoir which is separated from the Lower Shajara reservoir by an unconformity surface as revealed in Figure 1. It was nominated by four samples (Figure 1), three of which named as SJ7, SJ8, and SJ9 as illuminated in Table 1. Their positive slopes of the first procedure and negative slopes of the second procedure are shown in Figure 6, Figure 7 and Figure 8 and Table 1. Furthermore, their Thermo electric sensitivity fractal dimensions and capillary pressure fractal dimensions show similarities as defined in Table 1. Their fractal dimensions are higher than those of samples SJ3 and SJ4 from the Lower Shajara Reservoir due to an increase in their permeability as explained in table 1.

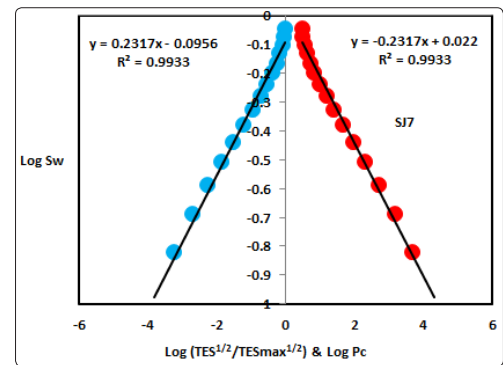


Figure 6:  $\text{Log} (TES^{1/2}/TES_{max}^{1/2})$  &  $\text{log pc}$  versus  $\text{log Sw}$  for sample SJ7

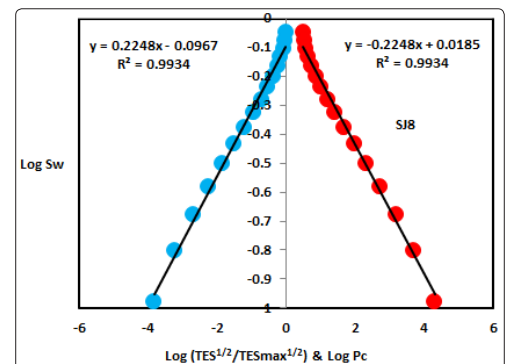


Figure 7:  $\text{Log} (TES^{1/2}/TES_{max}^{1/2})$  &  $\text{log pc}$  versus  $\text{log Sw}$  for sample SJ8

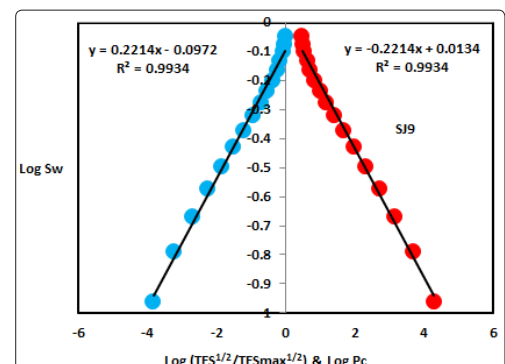
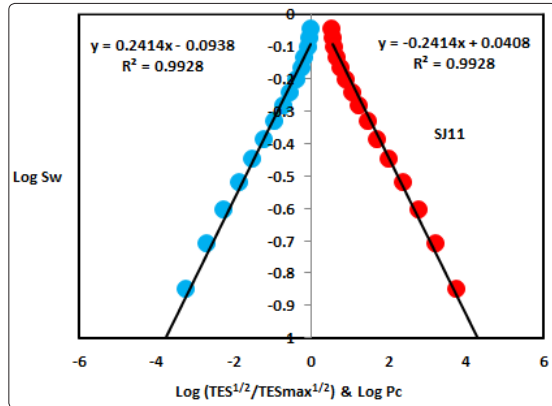
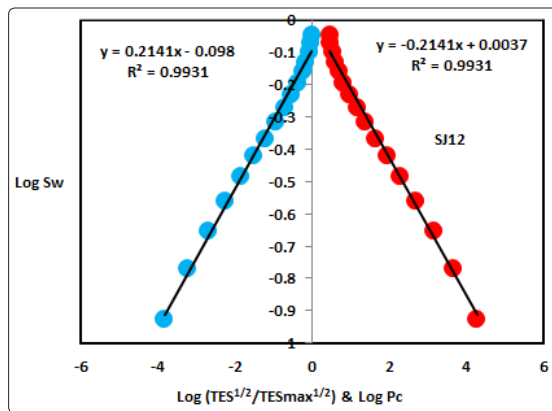


Figure 8:  $\text{Log} (TES^{1/2}/TES_{max}^{1/2})$  &  $\text{log pc}$  versus  $\text{log Sw}$  for sample SJ9

On the other hand, the Upper Shajara reservoir was separated from the Middle Shajara reservoir by yellow green mudstone as shown in Figure 1. It is defined by three samples so called SJ11, SJ12, SJ13 as explained in Table 1. Their positive slopes of the first procedure and negative slopes of the second procedure are displayed in Figure 9, Figure 10 and Figure 11 and Table 1. Moreover, their Thermo electric sensitivity fractal dimension and capillary pressure fractal dimension are also higher than those of sample SJ3 and SJ4 from the Lower Shajara Reservoir due to an increase in their permeability as simplified in table 1.



**Figure 9:** Log (TES<sup>1/2</sup>/TES<sub>max</sub><sup>1/2</sup>) & log pc versus log Sw for sample SJ11



**Figure 10:** Log (TES<sup>1/2</sup>/TES<sub>max</sub><sup>1/2</sup>) & log pc versus log Sw for sample SJ12

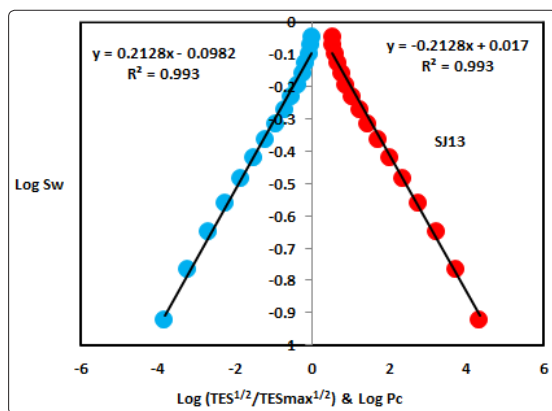


**Figure 11:** Log (TES<sup>1/2</sup>/TES<sub>max</sub><sup>1/2</sup>) & log pc versus log Sw for sample SJ13

Overall a plot of positive slope of the first procedure versus negative slope of the second procedure as described in Figure 12 reveals three permeable zones of varying Petrophysical properties. These reservoir zones were also confirmed by plotting Thermo electric sensitivity fractal dimension versus capillary pressure fractal dimension as described in Figure 13. Such variation in fractal dimension can account for heterogeneity which is a key parameter in reservoir quality assessment.

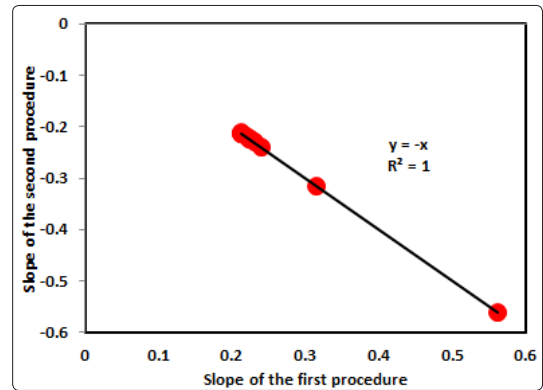


**Figure 12:** Slope of the first procedure versus slope of the second procedure

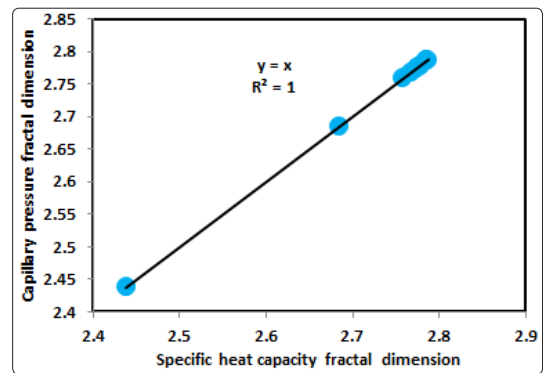


**Figure 13:** Thermo electric sensitivity fractal dimension versus capillary pressure fractal dimension

### Conclusion

The sandstones of the Shajara Reservoirs of the permo-Carboniferous Shajara Formation were divided here into three units based on Thermo electric sensitivity fractal dimension. The Units from base to top are: Lower Shajara Thermo Electric Sensitivity Fractal dimension Unit, Middle Shajara Thermo Electric Sensitivity Fractal Dimension Unit, and Upper Shajara Thermo Electric Sensitivity Fractal Dimension Unit. These units were also proved by capillary pressure fractal dimension. The fractal dimension was found to increase with increasing grain size and permeability owing to possibility of having interconnected channels.

### Acknowledgement

The author would to thank King Saud University, college of Engineering, Department of Petroleum and Natural Gas Engineering, Department of Chemical Engineering, Research Centre at College of Engineering, College of Science, Department of Geology, and King Abdullah Institute for research and Consulting Studies for their supports.



## References

1. Frenkel J (1944) on the theory of seismic and seismoelectric phenomena in a moist soil. *Journal of physics* 3: 230-241.
2. Li K, Williams W (2007) Determination of capillary pressure function from resistivity data. *Transport in Porous Media* 67: 1-15.
3. Revil A, Jardani A (2010) Seismoelectric response of heavy oil reservoirs: theory and numerical modelling. *Geophysical Journal Int* 180: 781-797.
4. Dukhin A, Goetz P, Thommes M (2010) Seismoelectric effect: a non-isochoric streaming current. I Experiment. *J Colloid Interface Sci* 345: 547-553.
5. Guan W, Hu H, Wang Z (2012) Permeability inversion from low-frequency seismoelectric logs in fluid-saturated porous formations. *Geophysical Prospecting* 61: 120-133.
6. Hu H, Guan W, Zhao W (2012) Theoretical studies of permeability inversion from seismoelectric logs. *Geophysical Research Abstracts* 14 : EGU2012-6725-1.
7. Borde C, S'en'echal P, Barri'ere J, D Brito, E Normandin, et al. (2015) Impact of water saturation on seismoelectric transfer functions: a laboratory study of co-seismic phenomenon. *Geophysical Journal International* 200: 1317-1335.
8. Jardani A, Revil A (2015) Seismoelectric couplings in a poroelastic material containing two immiscible fluid phases. *Geophys J Int* 202: 850-870.
9. Holzhauer J, Brito D, Bordes C, Y Brun, B Guatarbes (2016) Experimental quantification of the seismoelectric transfer function and its dependence on conductivity and saturation in loose sand. *Geophys Prospect* 65: 1097-1120.
10. Rong Peng, Jian-Xing Wei, Bang-Rang Di, Pin-Bo Ding, Zi-Chun Liu (2016) Experimental research on seismoelectric effects in sandstone. *Applied Geophysics* 13: 425-436.
11. Djuraev U, Jufar S R, Vasant P (2017) Numerical Study of frequency-dependent seismo electric coupling in partially-saturated porous media. *MATEC Web of Conferences* 87.
12. Alkhidir KEME (2017) Pressure head fractal dimension for characterizing Shajara Reservoirs of the Shajara Formation of the Permo-Carboniferous Unayzah Group, Saudi Arabia. *Archives of Petroleum and Environmental Biotechnology* 2: 1-7.
13. Al-Khidir KE (2018) On Similarity of Pressure Head and Bubble Pressure Fractal Dimensions for Characterizing Permo-Carboniferous Shajara Formation, Saudi Arabia. *Journal of Industrial Pollution and Toxicity* 1: 1-10.
14. Alkhidir KEME (2018) Geometric relaxation time of induced polarization fractal dimension for characterizing Shajara Reservoirs of the Shajara Formation of the Permo-Carboniferous Unayzah Group, Saudi Arabia. *Scifed J Petroleum* 2: 1-6.
15. Alkhidir KEME (2018) Geometric relaxation time of induced polarization fractal dimension for characterizing Shajara Reservoirs of the Shajara formation of the Permo-Carboniferous Unayzah Group-Permo. *International Journal of Petrochemistry and Research* 2: 105-108.

**Copyright:** ©2019 Khalid Elyas Mohamed Elameen Alkhidir. This is an open-access article distributed under the terms of the Creative Commons Attribution License, which permits unrestricted use, distribution, and reproduction in any medium, provided the original author and source are credited.